Multiband effects on β-FeSe single crystals

Hechang Lei (□□□), D. Graf, Rongwei Hu (□□□), Hyejin Ryu (□□□), E. S. Choi, S. W. Tozer, and C. Petrovic

Phys. Rev. B **85**, 094515 — Published 23 March 2012

DOI: 10.1103/PhysRevB.85.094515

Multiband effects on β-FeSe single crystals

Hechang Lei (雷和畅),[1] D. Graf,[2] Rongwei Hu (胡荣伟),[1,*] Hyejin Ryu,[1,3] E. S. Choi,[2] S. W. Tozer,[2] and C. Petrovic[1,3]
[1] *Condensed Matter Physics and Materials Science Department, Brookhaven National Laboratory, Upton, NY 11973, USA*
[2] *NHMFL/Physics, Florida State University, Tallahassee, Florida 32310, USA and*
[3] *Department of Physics and Astronomy, State University of New York at Stony Brook, Stony Brook, NY 11794, USA*
(Dated: February 14, 2012)

We present the upper critical fields $\mu_0 H_{c2}(T)$ and Hall effect in β-FeSe single crystals. The $\mu_0 H_{c2}(T)$ increases as the temperature is lowered for field applied parallel and perpendicular to (101), the natural growth facet of the crystal. The $\mu_0 H_{c2}(T)$ for both field directions and the anisotropy at low temperature increase under pressure. Hole carriers are dominant at high magnetic fields. However, the contribution of electron-type carriers is significant at low fields and low temperature. Our results show that multiband effects dominate $\mu_0 H_{c2}(T)$ and electronic transport in the normal state.

PACS numbers: 74.70.Xa, 74.25.Op, 74.62.Fj

I. INTRODUCTION

The discovery of iron-based superconductors has generated a great deal of interests because of rather high transition temperature T_c and high upper critical fields $\mu_0 H_{c2}$. Crystal structures of iron-based superconductors can be mainly categorized into several types: FePn-1111 type (REOFePn, RE = rare earth; Pn = P or As), FePn-122 type (AFe_2As_2, A = alkaline or alkaline-earth metals), FePn111 type (AFeAs), FeCh-11 type (FeCh, Ch = S, Se, Te), FeCh-122 type ($A_xFe_{2-y}Ch_2$), and other structures with more complex oxide layers.[1–6] Despite structural similarity, i.e., shared FePn or FeCh tetrahedron layers, iron-based superconductors exhibit diverse physical properties. These include possible differences in pairing symmetry,[7–10] relation to competing or coexisting order states (spin density wave vs. superconductivity),[11–13] and diverse normal state properties.[1,6] FeCh-11 type materials are of special interest because their crystal structure has no blocking layers in between FeCh layers, yet they have similar calculated Fermi surface topology when compared to other iron-based superconductors.[14] Furthermore, they also exhibit some exotic features, such as significant pressure effect,[15,16] and excess Fe with local moment according to theoretical calculation.[17]

The $\mu_0 H_{c2}$ gives some important information on fundamental superconducting properties: coherence length, anisotropy, details of underlying electronic structures and dimensionality of superconductivity as well as insights into the pair-breaking mechanism. Previous studies on $FeTe_{1-x}Se_x$ and $FeTe_{1-x}S_x$ single crystals indicate that the spin-paramagnetic effect is the main pair-breaking mechanism.[18–20] However, for FePn-1111 and FePn-122 type superconductors the two-band effect with high diffusivity ratio between different bands dominates $\mu_0 H_{c2}(T)$.[21–23]

On the other hand, magnetic penetration depth study of β-FeSe polycrystal indicates that β-FeSe is a two-band superconductor.[24] Therefore, it is of interest to investigate multiband and spin paramagnetic effects on the $\mu_0 H_{c2}$ of β-FeSe. An extremely complex binary alloy phase diagram and associated difficulties in single crystal preparation impeded the growth of pure β-FeSe single crystals.[25] Hence, systematic studies of anisotropy in $\mu_0 H_{c2}(T)$ and pair breaking mechanism in high magnetic field are still lacking.

In this work, we report on the upper critical fields of pure β-FeSe single crystals in dc high magnetic fields up to 35T at ambient and high pressures. The results shows that two-band features dominate the pair breaking with additional influence of spin paramagnetic effect.

II. EXPERIMENT

Details of crystal synthesis and characterization are explained elsewhere.[25] The $\mu_0 H_{c2}$ is determined by measuring the magnetic field dependence of radio frequency (rf) contactless penetration depth in a static magnet up to 35 T at the National High Magnetic Field Laboratory (NHMFL) in Tallahassee, Florida. The rf technique is very sensitive to small changes in the rf penetration depth (about 1-5 nm) in the mixed state and thus is an accurate method for determining the $\mu_0 H_{c2}$ of superconductors.[26] At certain magnetic field, the probe detects the transition to the normal state by tracking the shift in resonant frequency, which is proportional to the change in penetration depth as $\Delta\lambda \propto \Delta F$. Small single crystals were chosen and the sample was placed in a circular detection coil. More details can be found in Refs. 29 and 30. For measurement under pressure, the sample was placed in a 15 turn coil within the gasket hole of a turnbuckle diamond anvil cell (DAC) made of beryllium copper and containing diamonds with 1.2 mm culets.[27] The pressure was calibrated at $\sim$ 4 K by comparing the fluorescence of a small chip of ruby within the DAC with an ambient ruby at the same temperature.[28] The small dimensions of the DAC allow for angular rotation with respect to the applied magnetic field so H$\|$(101)

and H⊥(101) orientations can be explored *in situ*. Using four-probe configuration of Hall measurement, the Hall resistivity was extracted from the difference of transverse resistance measured at the positive and negative fields, i.e., $\rho_{xy}(H) = [\rho(+H) - \rho(-H)]/2$, which can effectively eliminate the longitudinal resistivity component due to voltage probe misalignment.

III. RESULTS AND DISCUSSION

As shown in the main panel of Fig. 1(a) and (b), the rf shift (ΔF) at 10 K (above T_c) shows a smooth and almost linear magnetic-field dependence without any steep changes for both field directions. In the normal state the rf shift is sensitive to the magnetoresistance of the sample and detection coil.[31] However, when the temperature is below T_c, there is a sudden increase of $\Delta F(H)$ which deviates from the background signal. This corresponds to entry to the mixed state. Moreover, with decreasing temperature, the inflexion points of the $\Delta F(H)$ curves shift to higher field for both field directions, consistent with the higher $\mu_0 H_{c2}(T)$ at lower temperature. The temperature dependence of $\mu_0 H_{c2}(T)$ for H‖(101) and H⊥(101) is determined from the intersections of $\Delta F(H)$ curves between the extrapolated slopes of the rf signals below inflexion points and the normal-state backgrounds ($T = 10$ K) (insets in Fig. 1(a) and (b)).[31] The difference between this and other criterion, e.g. the intersection of extrapolated slopes below and above inflexion points in each $\Delta F(H)$ curve, is taken as the error bar of $\mu_0 H_{c2}(T)$.

In order to compare the upper critical fields determined from different measurement methods, the $\mu_0 H_{c2}(T)$ obtained from $\Delta F(T, H)$ curves and $\rho(T, H)$ data with different criteria are plotted together (Fig. 2(a)).[32] In the low field region, the temperature dependence of $\mu_0 H_{c2}(T)$ determined from the rf shift is almost linear with slight upturn near $T_c(H = 0$ T). This is close to the $\mu_0 H_{c2,zero}(T)$ determined from 10% $\rho_n(T, H)$. It is consistent with the results reported in the literature.[33] Assuming $\mu_0 H_{c2}(T = 0.35$ K$) \approx \mu_0 H_{c2}(0)$, the zero temperature limit of upper critical fields are 17.4(2) and 19.7(4) T for H‖(101) and H⊥(101), respectively. On the other hand, according to the Werthamer-Helfand-Hohenberg (WHH) theory, orbital pair breaking field $\mu_0 H_{c2}(0) = -0.693 T_c (d\mu_0 H_{c2}/dT|_{T_c})$,[34] and using the initial slopes $d\mu_0 H_{c2}/dT|_{T_c}$ at low fields obtained from $\rho(T, H)$ data (-2.54(4) T/K for H‖(101) and -2.55(4) T/K for H⊥(101)) with $T_c = 8.7$ K,[32] we obtain the $\mu_0 H_{c2}(0)$ are 15.3(2) and 15.4(2) T for H‖(101) and H⊥(101), respectively. This is smaller than experimental results. The deviation from WHH model is clearly seen in Fig. 2(b), where the $\mu_0 H_{c2}(T)$ becomes gradually larger than expected values from theory. The enhancement of the $\mu_0 H_{c2}$ in the low temperature and high field region implies that multiband effect are not negligible. On the other hand, assuming the electron-phonon coupling parameter $\lambda_{e-ph} = 0.5$ (typical value for weak-coupling BCS superconductors),[35] the Pauli limiting field $\mu_0 H_p(0) = 1.86 T_c (1+\lambda_{e-ph})^{1/2}$ is 19.8 T.[36] This is nearly the same as the $\mu_0 H_{c2,H\perp(101)}(T =$ 0.35 K) and larger than values for H‖(101) or the orbital pair breaking fields. It suggests that the spin-paramagnetic effect might also have some influence on the upper critical fields. This is rather different from other FeCh-11 superconductors where the Pauli limiting fields are much smaller than orbital pair-breaking fields and therefore the spin-paramagnetic effect governs $\mu_0 H_{c2}(T)$.[19,20]

According to the two-band BCS model in the dirty limit with orbital pair breaking and negligible interband scattering,[37] $\mu_0 H_{c2}$ is given by

$$a_0[\ln t + U(h)][\ln t + U(\eta h)] + a_2[\ln t + U(\eta h)] + a_1[\ln t + U(h)] = 0 \quad (1)$$

where $t = T/T_c$, $U(x) = \psi(1/2 + x) - \psi(x)$, $\psi(x)$ the digamma function, $\eta = D_2/D_1$, D_1 and D_2 are intraband diffusivities of the bands 1 and 2, $h = H_{c2} D_1/(2\phi_0 T)$, ϕ_0 the magnetic flux quantum. a_0, a_1, and a_2 are constants described with intraband- and interband coupling strength, $a_0 = 2\varpi/\lambda_0$, $a_1 = 1 + \lambda_-/\lambda_0$, and $a_1 = 1 - \lambda_-/\lambda_0$, where $\varpi = \lambda_{11}\lambda_{22} - \lambda_{12}\lambda_{21}$, $\lambda_0 = (\lambda_-^2 + 4\lambda_{12}\lambda_{21})^{1/2}$, and $\lambda_- = \lambda_{11} - \lambda_{22}$. Terms λ_{11} and λ_{22} are the intraband couplings in the bands 1 and 2 and λ_{12} and λ_{21} describe the interband couplings between bands 1 and 2. It should be noted that if $\eta = 1$, eq. (1) will reduce to the simplified WHH equation for single-band dirty superconductors.[34] By using the coupling constants determined from an μSR experiment with very small interband coupling,[24] the combined $\mu_0 H_{c2,H\|(101)}(T)$ data from both rf and resistivity measurements can be very well explained (Fig. 2(a) fit lines). The ratio of band diffusivities is $\eta = 0.40$, which is similar to the value of FeAs-122 but much larger than that of other two-band iron-based superconductors, such as FeAs-1111.[21−23] With current coupling constants, it leads to the similar shape of $\mu_0 H_{c2,H\|(101)}(T)$ when compared to the FeAs-122,[23] but significantly different from FeAs-1111 where there is an obvious upturn at low temperature.[21,22] We have also performed fits for different values of coupling constants:[21−23] (1) dominant intraband coupling, $\varpi > 0$ and (2) dominant interband coupling, $\varpi < 0$. The different sets of fitting parameters result in almost identical result, fitting the experimental data well (Fig. 2(b)). The derived η is in the range of 0.32-0.44, suggesting that the fitting results are insensitive to the choice of coupling constants. Thus, either interband and intraband coupling strength are comparable or their difference is below the resolution of our experiment.

In order to further investigate multiband characteristics in β-FeSe, we studied the Hall effect of β-FeSe (Fig. 3). According to the band calculations, at least four bands originated from Fe 3d orbitals cross the Fermi level.[14] Two bands are hole type and the other two are

electron type.[14] We use a simplified two-carrier model including one electron type with electron density n_e and mobility μ_e and one hole type with hole density n_h and mobility μ_h. According to the classical expression for the Hall coefficient including both electron and hole type carriers,[38]

$$\rho_{xy}/\mu_0 H = R_H = \frac{1}{e}\frac{(\mu_h^2 n_h - \mu_e^2 n_e) + (\mu_h\mu_e)^2(\mu_0 H)^2(n_h - n_e)}{(\mu_e n_h + \mu_h n_e)^2 + (\mu_h\mu_e)^2(\mu_0 H)^2(n_h - n_e)^2} \quad (2)$$

Once there are two carrier types present, the field dependence of $\rho_{xy}(H)$ will become nonlinear. Moreover, eq. (2) gives $R_H = e^{-1} \cdot (\mu_h^2 n_h - \mu_e^2 n_e)/(\mu_e n_h + \mu_h n_e)^2$ when $\mu_0 H \to 0$, and $R_H = e^{-1} \cdot 1/(n_h - n_e)$ when $\mu_0 H \to \infty$. As shown in inset (a) of Fig. 3, $\rho_{xy}(H)$ is positive and almost linear in $\mu_0 H$ at T = 60 K, indicating the hole type carrier is dominant. However, $\rho_{xy}(H)$ exhibits obvious nonlinear behavior below 50 K and even changes sign in low fields at 15 K (inset (b) in Fig. 3). This is a signature of coexistence of electron and hole type carriers. The $\rho_{xy}(H)$ can be described very well using a linear relation for $T = 60$ K and eq. (2) for $T \leqslant 50$ K as shown with the solid fit lines in the inset (a) and (b) of Fig. 3. The obtained carrier density $n(= n_h - n_e)$ changes from 1.93×10^{21} cm^{-3} (15 K) to 4.7×10^{21} cm^{-3} (60 K) gradually. The change of sign of $\rho_{xy}(H)$ in the low field region at 15 K indicates $(\mu_h^2 n_h - \mu_e^2 n_e) < 0$. Because $n_h - n_e > 0$ at higher field, it indicates that the $\mu_e > \mu_h$ at low temperature, consistent with the band structure calculation results.[14] Moreover, the negative Seebeck coefficients in β-FeSe below ~ 250 K also confirm that the electron band is dominant at low temperature.[41]

Since there is remarkable pressure effect on T_c for β-FeSe,[15,16] it is instructive to study the pressure dependence of upper critical fields. As shown in the inset of Fig. 4, under pressure ($P = 0.51$ GPa), the inflexion point of $\Delta F(H)$ curve shifts to higher field when compared to the ambient pressure curve, suggesting that the $\mu_0 H_{c2}(T)$ is enhanced with pressure. It is consistent with the significant positive pressure effect of T_c for β-FeSe.[15,16] The temperature dependence of $\mu_0 H_{c2}(T)$ for H$\|$(101) and H$\perp$(101) shows that the upper critical fields for both field directions are enhanced in the whole measured temperature region under pressure. The $\mu_0 H_{c2}(T = 0.45$ K) for H$\perp$(101) is about 24.6 T, close to the estimated value at 1.48 GPa using linear extrapolation.[15] It suggests that $\mu_0 H_{c2}(0)$ at 0.51 GPa should be larger than linear-extrapolated value. This could originate from the difference in sample purity between our single crystals and polycrystals or intrinsic multiband effect. As shown in the inset (b) of Fig. 4, at ambient pressure, the anisotropy of $\mu_0 H_{c2}(T)$, $\gamma(P = 0$ GPa$, T) = \mu_0 H_{c2,H\perp(101)}(P = 0$ GPa$, T)/\mu_0 H_{c2,H\|(101)}(P = 0$ GPa$, T)$, is smaller than in other iron based superconductors, especially at high temperature. Moreover, the temperature dependence of $\gamma(P, T)$ increases at high temperature and decreases when $T \ll T_c$, which is different from other iron based superconductors in which the $\gamma(T)$ usually decreases with temperature. The increase of $\gamma(P, T)$ with temperature has also been observed in two-band superconductor MgB_2. This may be due to the higher contribution of the band with lower band anisotropy at low temperature. The decrease of $\gamma(P, T)$ with temperature when temperature is far from Tc may be related to the possible spin-paramagnetic effect. On the other hand, under pressure, the $\gamma(P = 0.51$ GPa$, T)$ increases when compared to the value at ambient pressure. This could originate from the pressure-induced Fermi surface changes that increase the anisotropy of Fermi velocity (diffusivity) of dominant band. It should be noted that in order to study the anisotropy and pressure evolution of $\mu_0 H_{c2}(T)$ more clearly, the pressure dependence of $\mu_0 H_{c2}(T)$ along crystallographic axes should be measured in the future.

IV. CONCLUSION

In summary, we studied the upper critical field of β-FeSe crystals. The results indicate that the two band effects dominate the $\mu_0 H_{c2}(T)$, with possible influence of spin-paramagnetic effect. A nonlinear field dependence of $\rho_{xy}(H)$ at low temperature also confirms the existence of multiple bands in electronic transport. The dominant carriers are hole-type in high field but electron type carriers become important in low field due to either increased carrier density or enhanced mobility. The $\mu_0 H_{c2}(T)$ is enhanced for both field directions and the anisotropy of $\mu_0 H_{c2}(0)$ is also increased under pressure.

V. ACKNOWLEDGEMENTS

Work at Brookhaven is supported by the U.S. DOE under Contract No. DE-AC02-98CH10886 (R. Hu and H. Ryu) and in part by the Center for Emergent Superconductivity, an Energy Frontier Research Center funded by the U.S. DOE, Office for Basic Energy Science (H. Lei and C. Petrovic). Work at the National High Magnetic Field Laboratory is supported by the DOE NNSA DEFG52-10NA29659 (S. W.T. and D. G.), by the NSF Cooperative Agreement No. DMR-0654118 and by the state of Florida.

*Present address: Center for Nanophysics & Advanced Materials and Department of Physics, University of Maryland, College Park MD 20742-4111, USA.

[1] Y. Kamihara, T. Watanabe, M. Hirano, and H. Hosono, J. Am. Chem. Soc. **130**, 3296 (2008).
[2] M. Rotter, M. Tegel, and D. Johrendt, Phys. Rev. Lett. **101**, 107006 (2008).
[3] X. C. Wang, Q. Q. Liu, Y. X. Lv, W. B. Gao, L. X. Yang, R. C. Yu, F. Y. Li, and C. Q. Jin, Solid State Commun. **148**, 538 (2008).
[4] X. Y. Zhu, F. Han, G. Mu, P. Cheng, B. Shen, B. Zeng, and H.-H. Wen, Phys. Rev. B **79**, 220512(R) (2009).
[5] F. C. Hsu, J. Y. Luo, K. W. Yeh, T. K. Chen, T. W. Huang, P. M. Wu, Y. C. Lee, Y. L. Huang, Y. Y. Chu, D. C. Yan, and M. K. Wu, Proc. Natl. Acad. Sci. U.S.A. **105**, 14262 (2008).
[6] J. Guo, S. Jin, G. Wang, S. Wang, K. Zhu, T. Zhou, M. He, and X. Chen, Phys. Rev. B **82**, 180520(R) (2010).
[7] I. I. Mazin, D. J. Singh, M. D. Johannes, and M. H. Du, Phys. Rev. Lett. **101**, 057003 (2008).
[8] H. Ding, P. Richard, K. Nakayama, K. Sugawara, T. Arakane, Y. Sekiba, A. Takayama, S. Souma, T. Sato, T. Takahashi, Z. Wang, X. Dai, Z. Fang, G. F. Chen, J. L. Luo, and N. L. Wang, EPL **83**, 47001 (2008).
[9] T. Hanaguri, S. Niitaka, K. Kuroki, and H. Takagi, Science **328**, 474 (2011).
[10] Y. Zhang, L. X. Yang, M. Xu, Z. R. Ye, F. Chen, C. He, H. C. Xu, J. Jiang, B. P. Xie, J. J. Ying, X. F. Wang, X. H. Chen, J. P. Hu, M. Matsunami, S. Kimura, and D. L. Feng, Nature Mater. **10**, 273 (2011).
[11] C. de la Cruz, Q. Huang, J. W. Lynn, J. Y. Li, W. Ratcliff II, J. L. Zarestky, H. A. Mook, G. F. Chen, J. L. Luo, N. L. Wang, and P. C. Dai, Nature **453**, 899 (2008).
[12] A. J. Drew, Ch. Niedermayer, P. J. Baker, F. L. Pratt, S. J. Blundell, T. Lancaster, R. H. Liu, G.Wu, X. H. Chen, I.Watanabe, V. K. Malik, A. Dubroka, M. Rössle, K. W. Kim, C. Baines, and C. Bernhard, Nature Mater. **8**, 310 (2009).
[13] H. Chen, Y. Ren, Y. Qiu, W. Bao, R. H. Liu, G. Wu, T. Wu, Y. L. Xie, X. F. Wang, Q. Huang, and X. H. Chen, EPL **85**, 17006 (2009).
[14] A. Subedi, L. Zhang, D. J. Singh, and M. H. Du, Phys. Rev. B **78**, 134514 (2008) .
[15] Y. Mizuguchi, F. Tomioka, S. Tsuda, T. Yamaguchi, and Y. Takano, Appl. Phys. Lett. **93**, 152505 (2008).
[16] S. Medvedev, T. M. McQueen, I. A. Troyan, T. Palasyuk, M. I. Eremets, R. J. Cava, S. Naghavi, F. Casper, V. Ksenofontov, G.Wortmann, and C. Felser, Nature Mater. **8**, 630 (2008).
[17] L. J. Zhang, D. J. Singh, and M. H. Du, Phys. Rev. B **79**, 012506 (2009).
[18] T. Kida, T. Matsunaga, M. Hagiwara, Y. Mizuguchi, Y. Takano, and K. Kindo, J. Phys. Soc. Jpn **78**, 113701 (2009).
[19] Hechang Lei, Rongwei Hu, E. S. Choi, J. B. Warren, and C. Petrovic, Phys. Rev. B **81**, 094518 (2010).
[20] Hechang Lei, Rongwei Hu, E. S. Choi, J. B. Warren, and C. Petrovic, Phys. Rev. B **81**, 184522 (2010).
[21] F. Hunte, J. Jaroszynski, A. Gurevich, D. C. Larbalestier, R. Jin, A. S. Sefat, M. A. McGuire, B. C. Sales, D. K. Christen, and D. Mandrus, Nature **453**, 903 (2008).
[22] J. Jaroszynski, F. Hunte, L. Balicas, Y.-J. Jo, I. Raičević, A. Gurevich, D. C. Larbalestier, F. F. Balakirev, L. Fang, P. Cheng, Y. Jia, and H. H. Wen, Phys. Rev. B **78**, 174523 (2008).
[23] S. A. Baily, Y. Kohama, H. Hiramatsu, B. Maiorov, F. F. Balakirev, M. Hirano, and H. Hosono, Phys. Rev. Lett. **102**, 117004 (2009).
[24] R. Khasanov, M. Bendele, A. Amato, K. Conder, H. Keller, H.-H. Klauss, H. Luetkens, and E. Pomjakushina, Phys. Rev. Lett. **104**, 087004 (2010).
[25] Rongwei Hu, Hechang Lei, M. Abeykoon, E. S. Bozin, S. J. L. Billinge, J. B. Warren, T. Siegrist, and C. Petrovic, Phys. Rev. B. **83**, 224502 (2011).
[26] C. Mielke, J. Singleton, M.-S. Nam, N. Harrison, C. C. Agosta, B. Fravel, and L. K. Montgomery, J. Phys. Condens. Matter **13**, 8325 (2001).
[27] D. E. Graf, R. L. Stillwell, K. M. Purcell, and S. W. Tozer, High Pressure Res. **31**, 533 (2011).
[28] J. D. Barnett, S. Block, and G.J. Piermarini, Rev. Sci. Instr. **44**, 1 (1973).
[29] T. Coffey, Z. Bayindir, J. F. DeCarolis, M. Bennett, G. Esper, and C. C. Agosta, Rev. Sci. Instrum. **71**, 4600 (2000).
[30] M. M. Altarawneh, C. H. Mielke, and J. S. Brooks, Rev. Sci. Instrum. **80**, 066104 (2009).
[31] M. M. Altarawneh, K. Collar, C. H. Mielke, N. Ni, S. L. Bud'ko, and P. C. Canfield, Phy. Rev. B **78**, 220505(R) (2008).
[32] Hechang Lei, Rongwei Hu, and C. Petrovic, Phys. Rev. B **84**, 014520 (2011).
[33] E. D. Mun, M. M. Altarawneh, C. H. Mielke, V. S. Zapf, R. Hu, S. L. Bud'ko, and P. C. Canfield, Phy. Rev. B **83**, 100514(R) (2011).
[34] N. R. Werthamer, E. Helfand, and P. C. Hohenberg, Phys. Rev. **147**, 295 (1966).
[35] P. B. Allen, in Handbook of Superconductivity, edited by C. P. Poole, Jr. (Academic Press, New York, 1999) p. 478.
[36] T. P. Orlando, E. J. McNiff, Jr., S. Foner, and M. R. Beasley, Phys. Rev. B **19**, 4545 (1979).
[37] A. Gurevich, Phys. Rev. B **67**, 184515 (2003).
[38] R. A. Smith, *Semiconductors*, Cambridge Univerisity Press, Cambridge, England, (1978).
[39] J. L. Zhang, L. Jiao, Y. Chen, H. Q. Yuan, arxiv: 1201.2548 (2011).
[40] L. Lyard, P. Szabó, T. Klein, J. Marcus, C. Marcenat, K. H. Kim, B.W. Kang, H. S. Lee, and S. I. Lee, Phy. Rev. Lett. **92**, 057001 (2004).
[41] T. M. McQueen, Q. Huang, V. Ksenofontov, C. Felser, Q. Xu, H. Zandbergen, Y. S. Hor, J. Allred, A. J. Williams, D. Qu, J. Checkelsky, N. P. Ong, and R. J. Cava, Phys. Rev. B **79**, 014522 (2009).

FIGURES

FIG. 1. Field dependence of frequency shift (ΔF) for (a) H$\|$(101) and (b) H$\perp$(101) at various temperatures. $\Delta F(T$ = 10 K) is set as a normal-state background signal. Inset (a) and (b): enlarged parts near the points that deviate from background signals. $\mu_0 H_{c2}(T)$ are determined from the interceptions between extrapolated straight lines below inflexion points and the curves of normal-state backgrounds for H$\|$(101) and H$\perp$(101), respectively. In the inset (a), the intersection of two slopes in $\Delta F(T = 6$ K) curve exhibits another criterion to determine the $\mu_0 H_{c2}(T)$ and the difference between two criterions is taken as the error bar of $\mu_0 H_{c2}(T)$.

FIG. 2. (a) Temperature dependence of $\mu_0 H_{c2}(T)$ of β-FeSe single crystal for H$\|$(101) (closed symbols) and H$\perp$(101) (open symbols) obtained from $\rho(T)$ and ΔF curves. (b) Fits of $\mu_0 H_{c2}(T)$ for H$\|$(101) using eq. (1) for different pairing scenarios: (1) WHH; (2) $\varpi > 0$, $\lambda_{11} = 0.241$, $\lambda_{22} = 0.195$, $\lambda_{12} = \lambda_{21} = 0.01$, $\eta = D_2/D_1 = 0.40$; (3) $\varpi > 0$, $\lambda_{11} = \lambda_{22}$ = 0.5, $\lambda_{12} = \lambda_{21} = 0.25$, $\eta = D_2/D_1 = 0.44$; (4) $\varpi > 0$, λ_{11} = 0.8 $\lambda_{22} = 0.34$, $\lambda_{12} = \lambda_{21} = 0.18$, $\eta = D_2/D_1 = 0.32$; and (5) $\varpi < 0$, $\lambda_{11} = \lambda_{22} = 0.49$, $\lambda_{12} = \lambda_{21} = 0.5$, $\eta = D_2/D_1 =$ 0.35;

FIG. 3. (a) Field dependence of $\rho_{xy}(H)$ at various temperatures. Solid lines are the fitting results using eq. (2). for $T < 60$ K and single-band model for $T = 60$ K. In order to exhibit data clearly, the $\rho_{xy}(H)$ at different temperatures are shifted along vertical axis with certain values. (b) Temperature dependence of carrier density $n(= n_h - n_e)$ of β-FeSe crystal.

FIG. 4. (a) Temperature dependence of $\mu_0 H_{c2}(T)$ for H$\|$(101) (closed symbols) and H$\perp$(101) (open symbols) at ambient pressure and $P = 0.51$ GPa obtained from ΔF curves. Inset (a) field dependence of ΔF at 0 and 0.51 GPa for H$\|$(101) at T = 0.35 K. Inset (b) The temperature dependence of the anisotropy of $\mu_0 H_{c2}(P, T)$ at $P = 0$ and 0.51 Gpa.

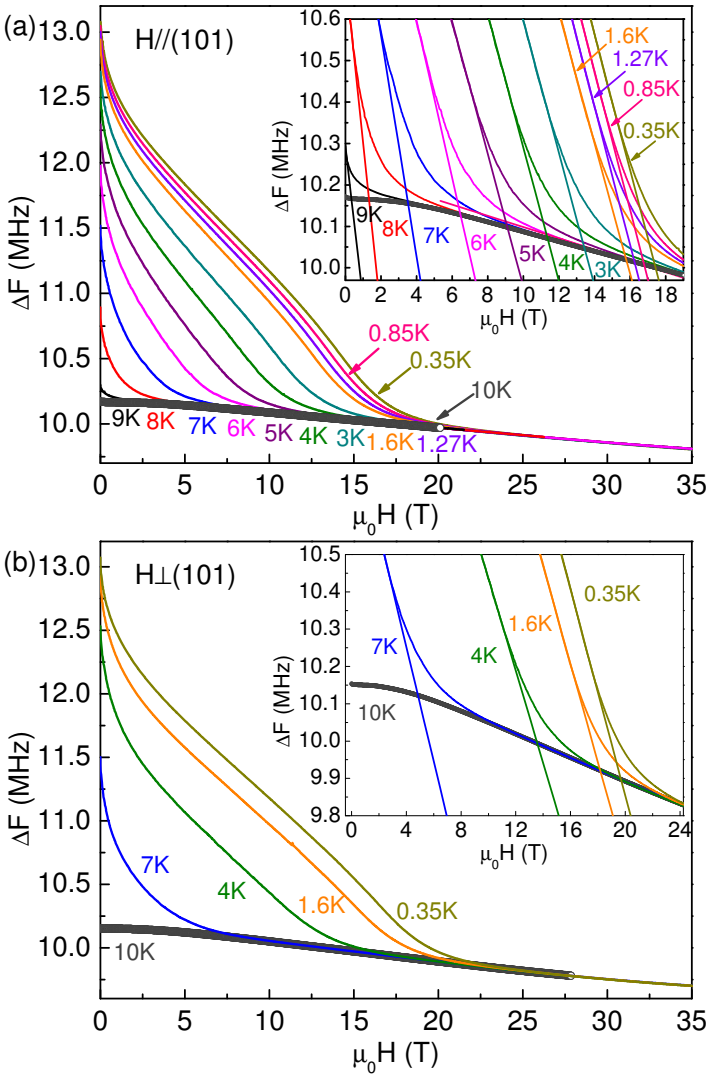

Figure 1 BM11912 14Feb2012

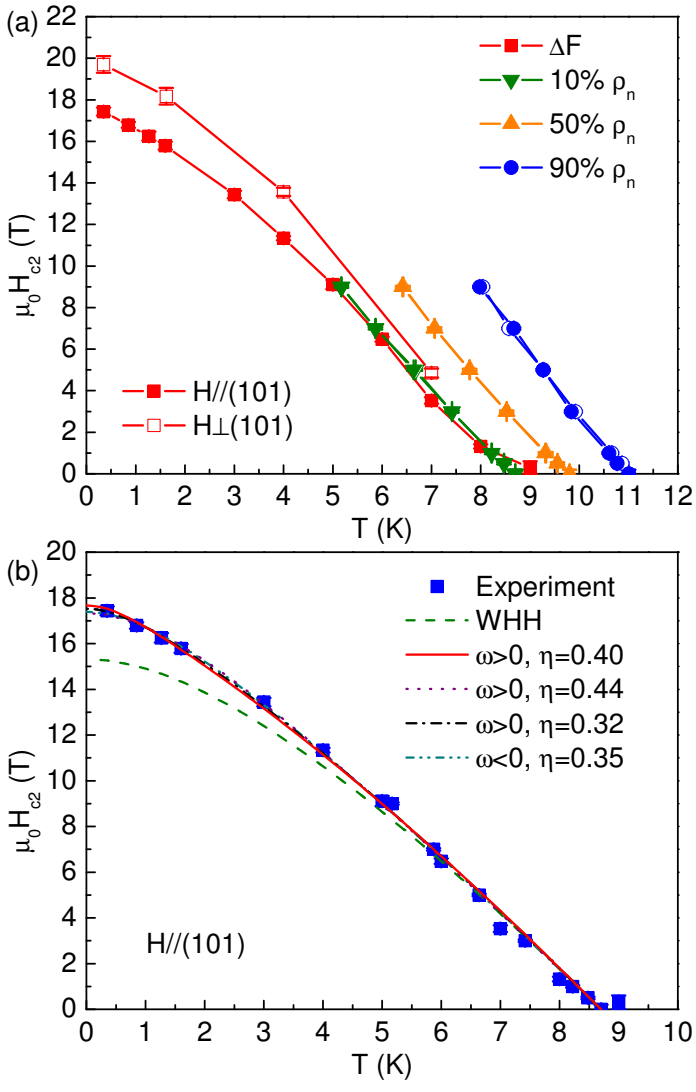

Figure 2 BM11912 14Feb2012

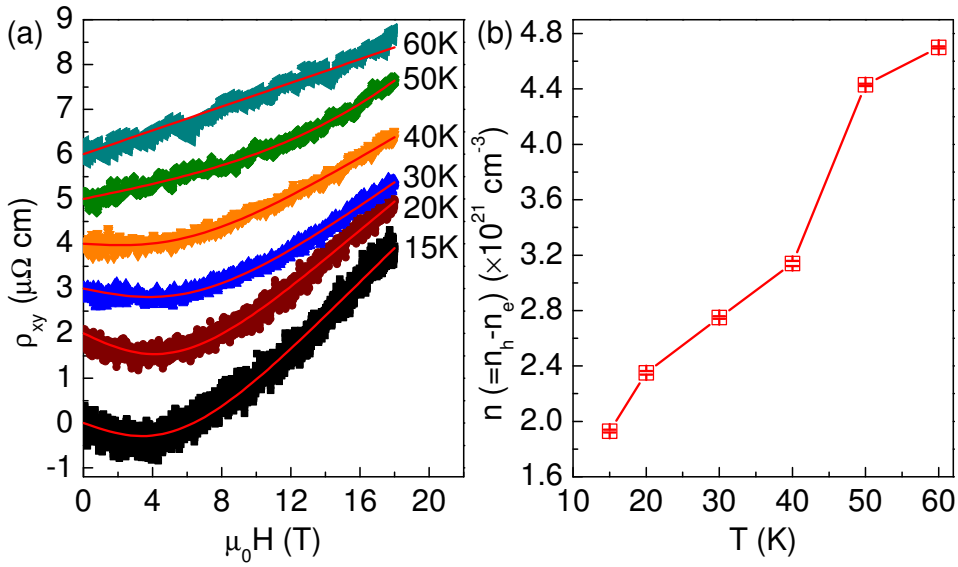

Figure 3 BM11912 14Feb2012

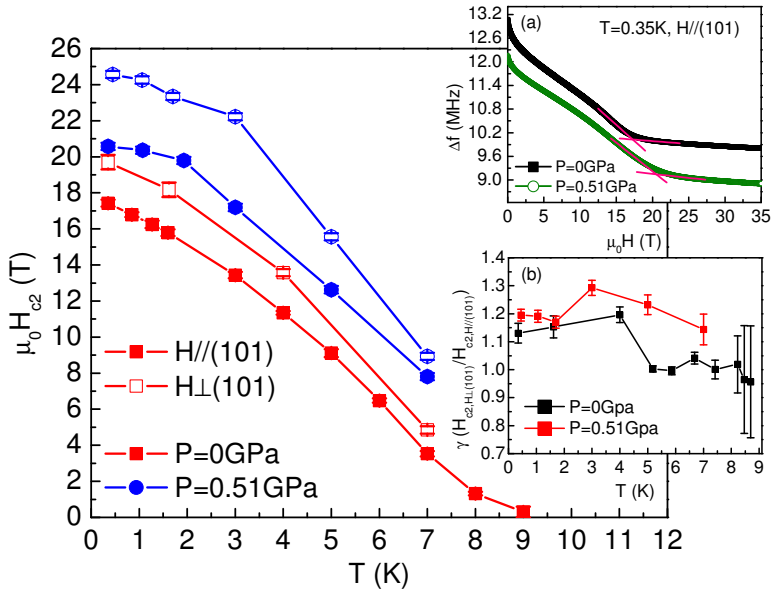

Figure 4 BM11912 14Feb2012